

Title: How do biological traits affect brachiopod taxonomic
2 survival? A hierarchical Bayesian approach.

Running title: How do biological traits affect taxonomic survival?

4 **Author:** Peter D Smits, psmits@uchicago.edu, Committee on Evolutionary
Biology, University of Chicago

6 **Keywords:** extinction, macroevolution, macroecology, Paleozoic, selection

Word count: ?

8 **Table count:** 0.

Figure count: 9 main text, 3 supplement.

10 **Data archival location:** Dryad.

Abstract

12 While the effect of geographic range on extinction risk is well
documented, the effects of other traits are less well known. Here, I analyze
14 patterns of Paleozoic brachiopod genus durations and their relationship to
geographic range, affinity for epicontinental seas versus open ocean
16 environments, and body size. Additionally, I allow for environmental
affinity to have a nonlinear effect on duration. Using a hierarchical
18 Bayesian modeling approach, I also model the possible interaction between
the effects of the biological traits and a taxon's time of origination. I find
20 evidence that as extinction risk increases, the expected strength of the
selection gradient on biological traits (except body size) increases. This
22 manifests as greater expected differences in extinction risk for each unit
change in geographic range and environmental preference during periods
24 of high extinction risk, as opposed to a much flatter expected selection
gradient during periods of low extinction risk. I find weak evidence for a
26 nonlinear relationship between environmental preference and extinction
risk such that "generalists" have a lower expected extinction risk than
28 either "specialists". Interestingly, I find that as extinction risk increases,
the peakedness of this relationship is expected to increase as well. These
30 results demonstrate the importance of directly modeling the structure
inherent in the observed data as a means to better understand which
32 processes may have been driving the observed patterns of diversification.

1 Introduction

34 How do biological traits affect extinction risk? Jablonski (1986) observed that
during periods of high expected extinction risk, the effects of biological traits on
36 survival decreased in importance. However, this pattern was weakest/absent in
the effect of geographic range on survival (Jablonski, 1986). Biological traits are

38 defined here as descriptors of a taxon’s adaptive zone, which is the set of
biotic–biotic and biotic–abiotic interactions that a taxon can experience. In
40 effect, these are descriptors of a taxon’s broad-sense ecology.

Jablonski (1986) phrased their conclusions in terms of background versus mass
42 extinction, but this scenario is readily transferable to a continuous variation
framework as there is no obvious distinction in terms of extinction rate between
44 these two states (Wang, 2003). I adopt a continuous variation framework as this
is more amenable for modeling the relationship between taxon traits and
46 extinction risk. Additionally, the Jablonski (1986) scenario has strong model
structure requirements in order to test its proposed macroevolutionary
48 mechanism. Not only do the taxon trait effects need to be modeled, but the
relationships between these effects need to be modeled as well.

50 Two possible macroevolutionary mechanisms which may underly the pattern
observed by Jablonski (1986) are: the effect of geographic range on predictive
52 survival remains constant and those of other biological traits decrease, and the
effect of geographic range in predicting survival increases and those of other
54 biological traits stay constant.

I model taxon durations because trait based differences in extinction risk should
56 manifest as differences in taxon durations. Namely, a species with a beneficial
trait should survive longer, on average, than a species without that beneficial
58 trait. Conceptually, taxon survival can be considered an aspect of “taxon fitness”
along with expected lineage branching/origination rate (Cooper, 1984, Palmer
60 and Feldman, 2012). The analysis of taxon durations, or time from origination
to extinction, falls under the purview of survival analysis, a field of applied
62 statistics commonly used in health care (Klein and Moeschberger, 2003) but has
a long history in paleontology (Simpson, 1944, 1953, Van Valen, 1973, 1979).

64 Geographic range is widely considered the most important taxon trait for
estimating differences in extinction risk at nearly all times with large geographic
66 range associated with low extinction risk (Jablonski, 1986, 1987, Jablonski and
Roy, 2003, Payne and Finnegan, 2007). I expect this to hold true nearly always.

68 The primary environmental dichotomy observed in ancient marine systems is
the contrast between epicontinental seas and open-ocean coastline environments
70 (Miller and Foote, 2009, Peters, 2008, Sheehan, 2001). Epicontinental seas are a
shallow-marine environment where, given a high enough sea-level, the ocean has
72 spread over the surface of a continental shelf with a depth typically less than
100m. In contrast, open-ocean coastline environments have much greater
74 variance in depth and do not cover the continental shelf. During the Paleozoic,
epicontinental seas were widely spread globally but declined over the Mesozoic
76 and eventually disappeared during the Cenozoic as open-ocean coastlines
became the dominant shallow-marine setting (Johnson, 1974, Miller and Foote,
78 2009, Peters, 2008).

Miller and Foote (2009) demonstrated that during several mass extinctions taxa
80 associated with open-ocean environments tend to have a greater extinction risk
than those taxa associated with epicontinental seas. During periods of
82 background extinction, however, they found no consistent difference between
taxa favoring either environment. Because of this study, the following prediction
84 for survival patterns can be made: as extinction risk increases, taxa associated
with open-ocean environments should generally increase in extinction risk versus
86 those that favor epicontinental seas.

There is also a possible nonlinear relationship between environmental preference
88 and taxon duration. A long standing hypothesis is that generalists or
unspecialized taxa will have greater survival than specialists (Baumiller, 1993,
90 Liow, 2004, 2007, Nürnberg and Aberhan, 2013, 2015, Simpson, 1944) SMITS,

IN PREP. I allowed for environmental preference to possibly have a parabolic
92 effect on species duration

Body size, measured as shell length (Payne et al., 2014), was also considered as
94 a potentially informative covariate. Body size is a proxy for metabolic activity
and other, correlated, life history traits (Payne et al., 2014). There is no strong
96 hypothesis of how body size effects extinction risk in brachiopods, meaning a
positive, negative, or null effect are all plausible.

98 I adopt a hierarchical Bayesian survival modeling approach, which represents a
conceptual and statistical unification of the paleontological dynamic and cohort
100 survival analytic approaches (Baumiller, 1993, Foote, 1988, Raup, 1975, 1978,
Simpson, 2006, Van Valen, 1973, 1979). By using a Bayesian framework I am
102 able to quantify the uncertainty inherent in the estimates of the effects of
biological traits on survival, especially in cases where the covariates of interest
104 (biological traits) are themselves known with error.

2 Materials and Methods

106 2.1 Fossil occurrence information

The dataset analyzed here was sourced from the Paleobiology Database
108 (<http://www.paleodb.org>) which was then filtered based on taxonomic,
temporal, stratigraphic, and other occurrence information that was necessary
110 for this analysis. These filtering criteria are very similar to those from Foote and
Miller (2013) with an additional constraint of being present in the body size
112 data set from Payne et al. (2014). Epicontinental versus open-ocean assignments
for each fossil occurrence are partially based on those from Miller and Foote
114 (2009), with additional occurrences assigned similarly (Miller and Foote,

personal communication).

116 Sampled occurrences were restricted to those with paleolatitude and
paleolongitude coordinates, assignment to either epicontinental or open-ocean
118 environment, and belonging to a genus present in the body size dataset (Payne
et al., 2014). Genus duration was calculated as the number of geologic stages
120 from first appearance to last appearance, inclusive. Genera with a last
occurrence in or after Changhsingian stage were right censored at the
122 Changhsingian. Genera with a duration of only one stage were left censored
(Appendix C). The covariates used to model genus duration were geographic
124 range size (r), environmental preference (v, v^2), and body size (m).

Geographic range was calculated using an occupancy approach. First, all
126 occurrences were projected onto an equal-area cylindrical map projection. Each
occurrence was then assigned to one of the cells from a 70×34 regular raster
128 grid placed on the map. Each grid cell represents approximately 250,000 km².
The map projection and regular lattice were made using shape files from
130 <http://www.natureearthdata.com/> and the **raster** package for R (Hijmans,
2015).

132 For each stage, the total number of occupied grid cells, or cells in which a fossil
occurs, was calculated. Then, for each genus, the number of grid cells occupied
134 by that genus was calculated. Dividing the genus occupancy by the total
occupancy gives the relative occupancy of that genus. Mean relative genus
136 occupancy was then calculated as the mean of the per stage relative occupancies
of that genus.

138 Body size data was sourced directly from Payne et al. (2014). Because those
measurements are presented without error, a measurement error model similar
140 to the one for environmental affinity could not be implemented (Appendix A).

Prior to analysis, geographic range and body size were transformed and
142 standardized in order to improve interpretability of the results. Geographic
range, which can only vary between 0 and 1, was logit transformed. Body size,
144 which is defined for all positive real values, was natural log transformed. These
covariates were then standardized by mean centering and dividing by two times
146 their standard deviation following Gelman and Hill (2007).

2.2 Analytical approach

148 Hierarchical modelling, sometimes called “mixed-effects modeling,” is a
statistical approach which explicitly takes into account the structure of the
150 observed data in order to model both the within and between group variance
(Gelman et al., 2013, Gelman and Hill, 2007). The units of study (e.g. genera)
152 each belong to a single grouping (e.g. origination cohort). These groups are
considered draws from a shared probability distribution (e.g. all cohorts,
154 observed and unobserved). The group-level parameters are then estimated
simultaneously as the other parameters of interest (e.g. covariate effects)
156 (Gelman et al., 2013). The subsequent estimates are partially pooled together,
where parameters from groups with large samples or effects remain large while
158 those of groups with small samples or effects are pulled towards the overall
group mean.

160 This partial pooling is one of the greatest advantages of hierarchical modeling.
By letting the groups “support” each other, parameter estimates then better
162 reflect our statistical uncertainty. Additionally, this partial pooling helps control
for multiple comparisons and possibly spurious results as effects with little
164 support are drawn towards the overall group mean (Gelman et al., 2013,
Gelman and Hill, 2007).

166 All covariate effects (regression coefficients), as well as the intercept term
 (baseline extinction risk), were allowed to vary by group (origination cohort).
 168 The covariance/correlation between covariate effects was also modeled. This
 hierarchical structure allows inference for how covariates effects may change
 170 with respect to each other while simultaneously estimating the effects
 themselves, propagating our uncertainty through all estimates.

172 Additionally, instead of relying on point estimates of environmental affinity, I
 treat environmental affinity as a continuous measure of the difference between
 174 the taxon’s environmental occurrence pattern and the background occurrence
 pattern (Appendix A).

176 **2.3 Survival model**

Genus durations were modeled as time-till-event data (Klein and Moeschberger,
 178 2003), with covariate information used in estimates of extinction risk as a
 hierarchical regression model. Genus durations were assumed to follow either an
 180 exponential or Weibull distribution. Each of these distributions makes
 assumptions about how duration may effect extinction risk (Klein and
 182 Moeschberger, 2003). The exponential distribution assumes that extinction risk
 is independent of duration. In contrast, the Weibull distribution allows for age
 184 dependent extinction via the shape parameter α , though only as a monotonic
 function of duration. Importantly, the Weibull distribution is equivalent to the
 186 exponential distribution when $\alpha = 1$.

The following variables are defined: y_i is the duration of genus i in geologic
 188 stages, X is the matrix of covariates including a constant term, B_j is the vector
 of regression coefficients for origination cohort j , Σ is the covariance matrix of
 190 the regression coefficients, τ is the vector of scales the standard deviations of

the between-cohort variation in regression coefficient estimates, and Ω is the
192 correlation matrix of the regression coefficients.

The exponential model is defined

$$\begin{aligned}
y_i &\sim \text{Exponential}(\lambda) \\
\lambda_i &= \exp(\mathbf{X}_i B_{j[i]}) \\
B &\sim \text{MVN}(\vec{\mu}, \Sigma) \\
\Sigma &= \text{Diag}(\vec{\tau}) \Omega \text{Diag}(\vec{\tau}) \\
\mu_k &\sim \begin{cases} \mathcal{N}(0, \psi_k \lambda) & \text{if } k \neq r, \text{ or} \\ \mathcal{N}(-1, 1) & \text{if } k = r \end{cases} \\
\tau_k &\sim \text{C}^+(1) \\
\psi_k &\sim \text{C}^+(1) \\
\lambda &\sim \text{C}^+(1) \\
\Omega &\sim \text{LKJ}(2).
\end{aligned} \tag{1}$$

194 Similarly, the Weibull model is defined

$$\begin{aligned}
y_i &\sim \text{Weibull}(\alpha, \sigma) \\
\sigma_i &= \exp\left(\frac{-(\mathbf{X}_i B_{j[i]})}{\alpha}\right) \\
B &\sim \text{MVN}(\vec{\mu}, \Sigma) \\
\Sigma &= \text{Diag}(\vec{\tau})\Omega\text{Diag}(\vec{\tau}) \\
\alpha &\sim \text{C}^+(2) \\
\mu_k &\sim \begin{cases} \mathcal{N}(0, \psi_k \lambda) & \text{if } k \neq r, \text{ or} \\ \mathcal{N}(-1, 1) & \text{if } k = r \end{cases} \quad (2) \\
\tau_k &\sim \text{C}^+(1) \\
\psi_k &\sim \text{C}^+(1) \\
\lambda &\sim \text{C}^+(1) \\
\Omega &\sim \text{LKJ}(2).
\end{aligned}$$

The principle difference between this model and the previous (Eq. 1) is the
196 inclusion of the shape parameter α . Note that σ is approximately equivalent to
 $1/\lambda$.

198 For an explanation of how this model was developed, parameter explanations,
and choice of priors, please see Appendix B. Note that these models (Eq. 1, 2)
200 do not include how the uncertainty in environmental affinity is included nor how
censored observations are included. For an explanation of both of these aspects,
202 see Appendices A and C.

2.4 Parameter estimation

204 The joint posterior was approximated using a Markov-chain Monte Carlo
routine that is a variant of Hamiltonian Monte Carlo called the No-U-Turn
206 Sampler (Hoffman and Gelman, 2014) as implemented in the probabilistic
programming language Stan (Stan Development Team, 2014a). The posterior
208 distribution was approximated from four parallel chains run for 10,000 draws
each, split half warm-up and half sampling and thinned to every 10th sample for
210 a total of 5000 posterior samples. Chain convergence was assessed via the scale
reduction factor \hat{R} where values close to 1 ($\hat{R} < 1.1$) indicate approximate
212 convergence. Convergence means that the chains are approximately stationary
and the samples are well mixed (Gelman et al., 2013).

2.5 Model evaluation

Models were evaluated using both posterior predictive checks and an estimate of
216 out-of-sample predictive accuracy. The motivation behind posterior predictive
checks as tools for determining model adequacy is that replicated data sets
218 using the fitted model should be similar to the original data (Gelman et al.,
2013). Systematic differences between the simulations and observations indicate
220 weaknesses of the model fit. An example of a technique that is very similar
would be inspecting the residuals from a linear regression.

222 The strategy behind posterior predictive checks is to draw simulated values
from the joint posterior predictive distribution, $p(y^{rep}|y)$, and then compare
224 those draws to the empirically observed values (Gelman et al., 2013). To
accomplish this, for each replicate, a single value is drawn from the marginal
226 posterior distributions of each regression coefficient from the final model as well
as α for the Weibull model (Eq. 1, 2). Then, given the covariate information \mathbf{X} ,

228 a new set of n genus durations are generated giving a single replicated data set
 y^{rep} . This is repeated 1000 times in order to provide a distribution of possible
230 values that could have been observed given the model.

In order to compare the fitted model to the observed data, various graphical
232 comparisons or test quantities need to be defined. The principal comparison
used here is a comparison between non-parameteric approximation of the
234 survival function $S(t)$ as estimated from both the observed data and each of the
replicated data sets. The purpose of this comparison is to determine if the
236 model approximates the same survival/extinction pattern as the original data.

The exponential and Weibull models were compared for out-of-sample predictive
238 accuracy using the widely-applicable information criterion (WAIC) (Watanabe,
2010). Out-of-sample predictive accuracy is a measure of the expected fit of the
240 model to new data. However, because the Weibull model reduces to the
exponential model when $\alpha = 1$ my interest is not in choosing between these
242 models. Instead, comparisons of WAIC values are useful for better
understanding the effect of model complexity on out-of-sample predictive
244 accuracy. The calculation of WAIC used here corresponds to the “WAIC 2”
formulation recommended by Gelman et al. (2013). For an explanation of how
246 WAIC is calculated, see Appendix D. Lower values of WAIC indicate greater
expected out-of-sample predictive accuracy than higher values.

248 **3 Results**

As stated above, posterior approximations for both the exponential and Weibull
250 models achieved approximate stationarity after 10,000 steps, as all parameter
estimates have an $\hat{R} < 1.1$.

252 Comparisons of the survival functions estimated from 1000 posterior predictive
data sets to the estimated survival function of the observed genera demonstrates
254 that both the exponential and Weibull models approximately capture the
observed pattern of extinction (Fig. 1). The major difference in fit between the
256 two models is that the Weibull model has a slightly better fit for longer lived
taxa than the exponential model.

258 Additionally, the Weibull model is expected to have slightly better out-of-sample
predictive accuracy when compared to the exponential model (WAIC 4577
260 versus 4605, respectively). 1). Because the difference in WAIC between these
two models is large, while results from both the exponential and Weibull models
262 will be presented, only those from the Weibull model will be discussed.

Estimates of the overall mean covariate effects μ can be considered
264 time-invariant generalizations for brachiopod survival during the Paleozoic
SMITS IN PREP (Fig. 2). Consistent with prior expectations, geographic range
266 size has a negative effect on extinction risk, where genera with large ranges
having greater durations than genera with small ranges.

268 I find that there is an approximately 93% posterior probability that the overall
effect of increasing body size decreases expected extinction risk. This parameter,
270 however, is not very large and is within two standard deviations of 0 (mean
 $\mu_m = -0.15$, standard deviation 0.1). Because of this, I interpret this as weak
272 evidence for increases in body size to be associated with a decrease in expected
extinction risk.

274 Interpretation of the effect of environmental preference v on duration is slightly
more involved. Because a quadratic term is the equivalent of an interaction
276 term, both μ_v and μ_{v^2} have to be interpreted together because it is illogical to
change values of v without also changing values v^2 . To determine the nature of

278 the effect of v on duration I calculated the multiplicative effect of environmental
preference on extinction risk.

280 Given mean estimated extinction risk $\tilde{\sigma}$, we can define the extinction risk
multiplier of an observation with environmental preference v_i as

$$\frac{\tilde{\sigma}_i}{\tilde{\sigma}} = f(v_i) = \exp\left(\frac{-(\mu_v v_i + \mu_{v^2} v_i^2)}{\alpha}\right). \quad (3)$$

282 This function $f(v_i)$ has a y-intercept of $\exp(0)$ or 1 because it does not have a
non-zero intercept term. Equation 3 can be either concave up or down. A
284 concave down $f(v_i)$ may indicate that genera of intermediate environmental
preference have greater durations than either extreme, and *vice versa* for
286 concave up function.

The expected effect of environmental preference as a multiplier of expected
288 extinction risk can then be visualized (Fig. 3). This figure depicts 1000 posterior
predictive estimates of Eq. 3 across all possible values of v . The number
290 indicates the posterior probability that the function is concave down, with
generalists having lower extinction risk/greater duration than either type of
specialist. Note that the inflection point/optimum of Fig. 3 is approximately
292 $x = 0$, something that is expected given the estimate of μ_v (Fig. 2).

294 The matrix Σ describing the covariance between the different coefficients
describes how these coefficients might vary together across the origination
296 cohorts. Similar to how this was modeled (Eq. 1, 2), for interpretation purposes
 Σ can be decomposed into a vector of standard deviations $\vec{\tau}$ and a correlation
298 matrix Ω .

The estimates of the standard deviation of between-cohort coefficient estimates
300 τ indicate that some effects can vary greatly between-cohorts (Fig. 4).
Coefficients with greater values of τ have greater between-cohort variation. The

302 covariate effects with the greatest between origination cohort variation are β_r ,
 β_v , and β_{v^2} . Estimates of β_m have negligible between cohort variation, as there
304 is less between cohort variation than the between cohort variation in baseline
extinction risk β_0 . However the amount of between cohort variation in estimates
306 of β_{v^2} means that it is possible for the function describing the effect of
environmental affinity to be upward facing for some cohorts (Eq. 3), which
308 corresponds to environmental generalists being shorted lived than specialists in
that cohort.

310 The correlation terms of Ω (Fig. 5) describe the relationship between the
coefficients and how their estimates may vary together across cohorts. The
312 correlations between the intercept term β_0 and the effects of the taxon traits are
of particular interest for evaluating the Jablonski (1986) scenario (Fig. 5 first
314 column/last row). Keep in mind that when β_0 is low, extinction risk is low; and
conversely, when β_0 is high, then extinction risk is high.

316 Marginal posterior probabilities of the correlations between the level of baseline
extinction risk β_0 and the effects of the taxon traits indicate that the correlation
318 between expected extinction risk and both geographic range β_r and β_{v^2} are of
particular note (Fig. 6).

320 There is approximately a 98% probability that β_0 and β_r are negatively
correlated (Fig. 6), meaning that as extinction risk increases, the
322 effect/importance of geographic range on genus duration increases. This means
that increases in baseline extinction rate are correlated with an increased
324 importance of geographic range size. There is a 94% probability that β_0 and β_{v^2}
are negatively correlated (Fig. 6), meaning that as extinction risk increases, the
326 peakedness of $f(v_i)$ increases and the relationship tends towards concave down.
Additionally, there is a 97% probability that values of β_r and β_{v^2} are positively
328 correlated (Mean correlation 0.51, standard deviation 0.23).

While the overall group level estimates are of particular importance when
 330 defining time-invariant differences in extinction risk, it is also important and
 useful to analyze the individual level parameter estimates in order to better
 332 understand how parameters actually vary across cohorts.

In comparison to the overall mean extinction risk μ_0 , cohort level estimates β_0
 334 show some amount of variation through time as expected by estimates of τ_0
 (Fig. 7). A similar, if slightly greater, amount of variation is also observable in
 336 cohort estimates of the effect of geographic range β_r (Fig. 8). Again, smaller
 values of β_0 correspond to lower expected extinction risk. Similarly, smaller
 338 values of β_r correspond to greater decrease in extinction risk with increasing
 geographic range

How the effect of environmental affinity varies between cohorts can be observed
 340 by using the cohort specific coefficients estimates. Following the same procedure
 by using the cohort specific estimates of β_v and β_{v^2} for
 342 μ_v and μ_{v^2} , the cohort specific effect of environmental preference as a multiplier
 of mean extinction risk can be calculated. This was done only for the Weibull
 344 model, though the observed pattern should be similar for the exponential model.

As expected based on the estimates of τ_v and τ_{v^2} , there is greater variation in
 346 the peakedness of $f(v_i)$ than there is variation between concave up and down
 functions (Fig. 9). 9 of the 33 cohorts have less than 50% posterior probability
 348 that generalists are potentially expected to be shorter lived than specialists,
 though two of those cases have approximately a 50% probability of being either
 350 concave up or down. This is congruent with the 0.86 posterior probability that
 352 μ_{v^2} is positive/ $f(v_i)$ is concave down.

Additionally, for some cohorts there is a quite striking pattern where the effect
 354 of environmental preference v has a nearly-linear relationship (Fig. 9). These are

primarily scenarios where one of the end member preferences is expected to
 356 have a greater duration than either intermediate or the opposite end member
 preference. Whatever curvature is present in these nearly-linear cases is due to
 358 the definition of $f(v)$ as it is not defined for non-negative values of σ (Eq. 3). For
 most of the all stages between the Emsian through the Tournaisian, inclusive,
 360 intermediate preferences are of intermediate extinction risk when compared with
 epicontinental specialists (lowest risk) or open-ocean specialists (highest risk).
 362 This time period represents most of the Devonian.

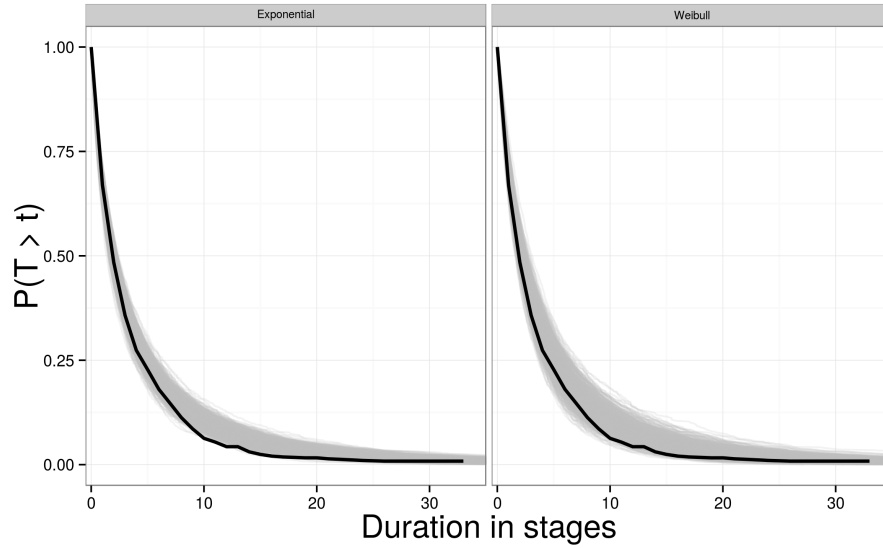


Figure 1: Comparison of empirical estimates of $S(t)$ versus estimates from 1000
 posterior predictive data sets. $S(t)$ corresponds to $P(T > t)$ as it is the probability
 that a given genus observed at age t will continue to live. This is equivalent to
 the probability that t is less than the genus' ultimate duration T . Note that the
 Weibull (left) model has noticeably better fit to the data than the exponential
 (right).

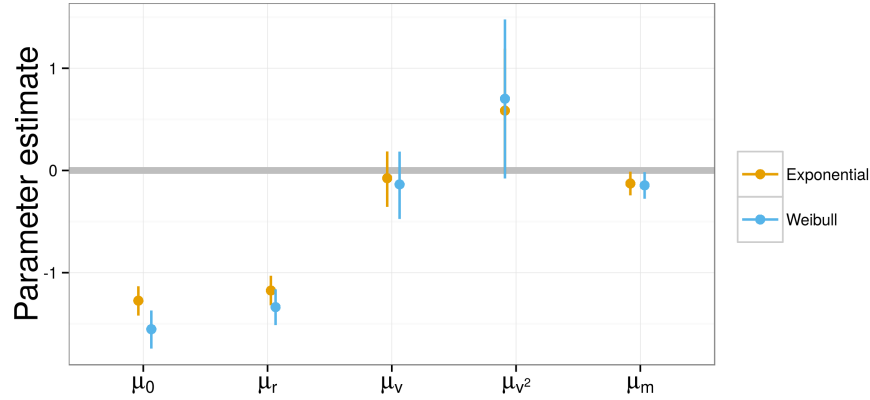


Figure 2: Estimates of the overall effects of the covariates on extinction risk. Included is also the estimate of μ_0 which corresponds to the intercept term or, because of standardization, the overall mean expected extinction risk. Estimates are presented for both the exponential (gold) and Weibull (blue) models. The point corresponds to the median of the posterior distribution, while the error bars correspond to the 80% credible intervals of the estimates.

4 Discussion

My results demonstrate that both the effects of geographic range and the peakedness/concavity of environmental preference are both negatively correlated with baseline extinction risk, meaning that as baseline extinction risk increases the effect sizes of both these traits are expected to increase (Fig. 6). This result supports neither of the two proposed macroevolutionary mechanisms for how biological traits should correlate with extinction risk. The observed correlation between the two effects as well as between the effects and baseline extinction risk instead implies that as baseline extinction risk increases, the strength of the total selection gradient on biological traits (except body size) increases. This manifests as greater differences in extinction risk for each unit difference in the biological covariates during periods of high extinction risk, while a relatively flatter selection gradient during periods of low extinction risk.

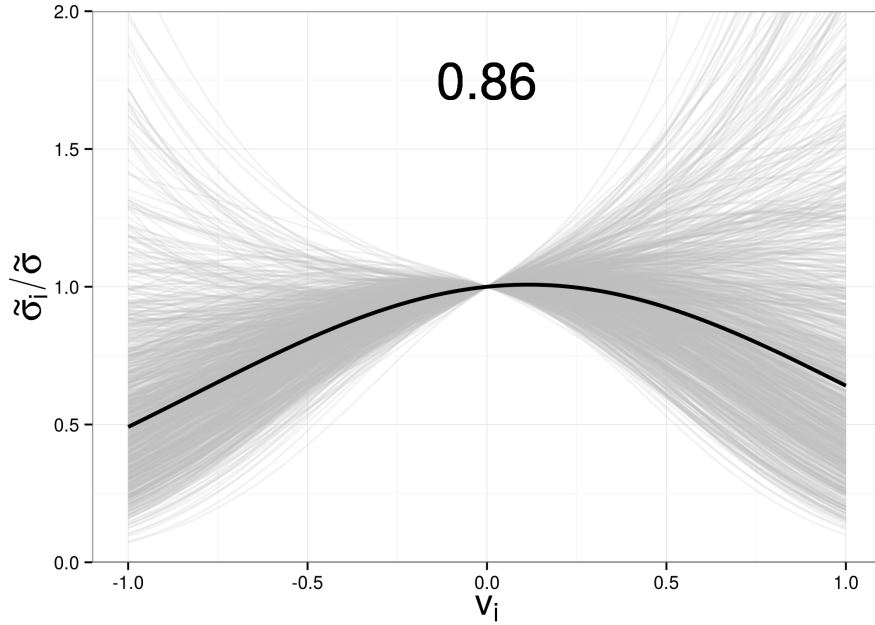


Figure 3: The overall expected relationship $f(v_i)$ between environmental affinity v_i and a multiplier of extinction risk (Eq. 3). Each grey line corresponds to a single draw from the posterior predictive distribution, while the black corresponds to the median of the posterior predictive distribution. The overall shape of $f(v_i)$ is concave down with an optimum of close 0, which corresponds to affinity approximately equal to the expectation based on background environmental occurrence rates.

376 There are two mass extinction events that are captured within the time frame
 considered here: the Ordovician-Silurian and the Frasnian-Famennian. The
 378 cohorts bracketing these events are worth considering in more detail.

The proposed mechanism for the end Ordovician mass extinction is a decrease
 380 in sea level and the draining of epicontinental seas due to protracted glaciation
 (Johnson, 1974, Sheehan, 2001). My results are broadly consistent with this
 382 scenario with both epicontinental and open-ocean specialists having a much
 lower expected duration than intermediate taxa (Fig. 9). All of the stages
 384 between the Darriwillian and the Llandovery, except the Hirnantian, have a

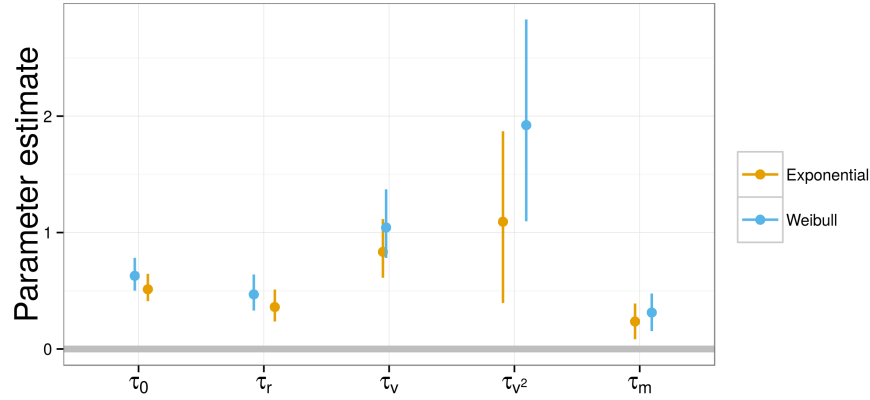


Figure 4: Estimates of the scale parameters describing the expected differences in the effect of the covariates, and of the intercept/baseline extinction risk, between cohorts. Higher values of τ correspond to greater expected differences between cohorts. Estimates are presented for both the exponential (gold) and Weibull (blue) models. The point corresponds to the median of the posterior distribution, while the error bars correspond to the 80% credible intervals of the estimates.

greater than expected probability that $f(v)$ is concave down. The pattern for the Darriwilian, which marks the supposed start of Ordovician glacial activity, demonstrates that taxa tend to favor open-ocean environments are expected to have a greater duration than either intermediate or epicontinental specialists, in decreasing order.

For nearly the entire Devonian estimates of $f(v)$ indicate that one of the environmental end members is favored over the other end member of intermediate preference (Fig. 9). This is consistent with Miller and Foote (2009). For the Givetian though the end of the Devonian and into the Tournaisian, I find that epicontinental favoring taxa are expected to have a greater duration than either intermediate or open-ocean specialists. Additionally, for nearly the entire Devonian except the Eifelian and through the Viséan, the cohort-specific estimates of $f(v)$ are concave-up. This is the opposite pattern than what is

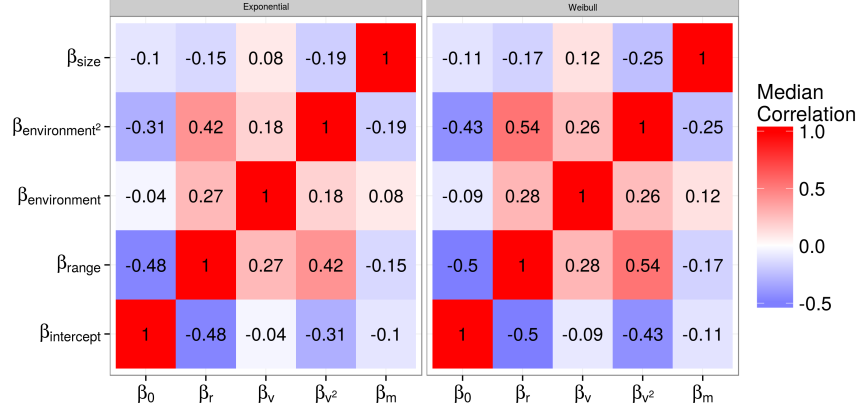


Figure 5: Heatmap for the median estimates of the terms of the correlation matrix Ω between cohort-level covariate effects. Both the exponential (left) and Weibull (right) models are presented. The off-diagonal terms are the correlation between the estimates of the cohort-level estimates of the effects of covariates, along with intercept/baseline extinction risk.

398 expected (Fig. 3). This result, however, seems to reflect the intensity of the
seemingly nearly-linear difference in expected duration across the range of v) as
400 opposed to an inversion of the weakly expected curvilinear pattern.

There is an approximate 86% posterior probability that taxa with intermediate
402 environmental preferences are possibly expected to have a lesser extinction risk
than either end members, the over all curvature of $f(v_i)$ is not very peaked,
404 meaning that this relationship does not lead to very strong differences in
extinction risk (Fig. 3). This result gives weak support for the hypothesis that,
406 in general, environmental generalists survive for longer than environmental
specialists (Liow, 2004, 2007, Nürnberg and Aberhan, 2013, 2015, Simpson,
408 1944).

The variance in estimate of the overall $f(v_i)$ reflects the large between cohort
410 variance in cohort specific estimates of $f(v_i)$ (Fig. 9). Given that there is only a
86% posterior probability that the expected overall estimate of $f(v_i)$ is concave

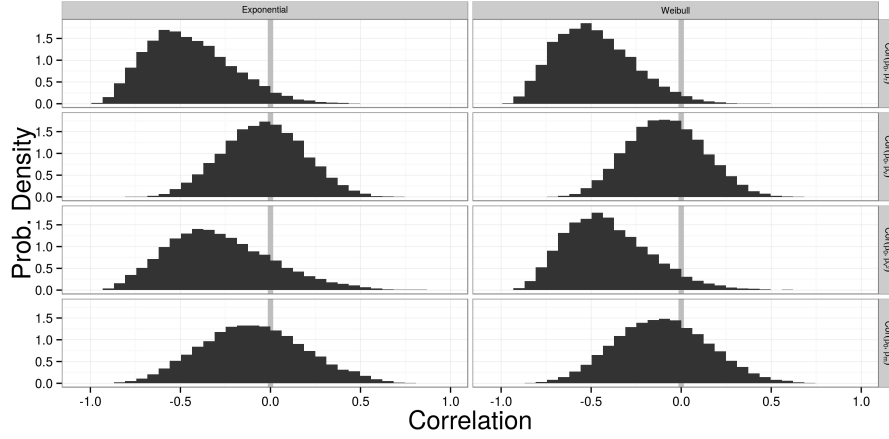


Figure 6: Marginal posterior distributions of the correlations between intercept terms/baseline extinction risk and the effects of each of the covariates. These are presented for both the exponential (left) and Weibull (right) models.

412 down, it is not surprising that there are some stages where the theorized
relationship is in fact reversed. Additionally, as discussed earlier, some of those
414 same stages where $f(v_i)$ does not resemble the theorized nonlinear relation with
the optimum in the middle, but are instead is highly skewed or effectively linear
416 (Fig. 9).

These results do not necessarily refute “survival of the unspecialized” as a
418 time-invariant generalization, but instead demonstrate how, while the expected
group-level estimate of $f(v_i)$ might favor one hypothesis, there is still enough
420 variability between cohorts so that in some realizations this pattern may not
hold or can even be reversed. These results are also consistent with aspects of
422 Miller and Foote (2009) who found that the effect of environmental preference
on extinction risk was quite variable and without obvious patterning during
424 times of background extinction.

This model can be improved through either increasing the number of analyzed
426 taxon traits, expanding the hierarchical structure of the model to include other

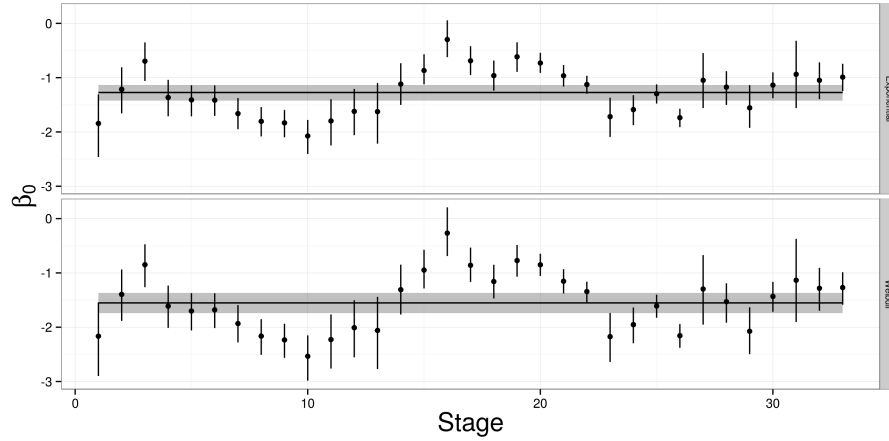


Figure 7: Comparison of cohort-specific estimates of β_0 presented along with the estimate for the overall baseline extinction risk. Points correspond to the median of the cohort-specific estimate, along with 80% credible intervals. The horizontal line is the median estimate of the overall baseline extinction risk along with 80% credible intervals. Results are presented for the exponential (top) and Weibull (bottom) models.

major taxonomic groups of interest, and the inclusion of explicit phylogenetic
relationships between the taxa in the model as an additional hierarchical effect.

An example taxon trait that may be of particular interest is the affixing
strategy or method of interaction with the substrate of the taxon. This trait has
been found to be related to brachiopod survival (Alexander, 1977) so its
inclusion may be of particular interest.

It is theoretically possible to expand this model to allow for comparisons within
and between major taxonomic groups. This approach would better constrain the
brachiopod estimates while also allowing for estimation of similarities and
differences in cross-taxonomic patterns. The major issue surrounding this
particular expansion involves finding an similarly well sampled taxonomic group
that is present during the Paleozoic. Example groups include Crinoidea,
Ostracoda, and other “Paleozoic” groups (Sepkoski Jr., 1981).

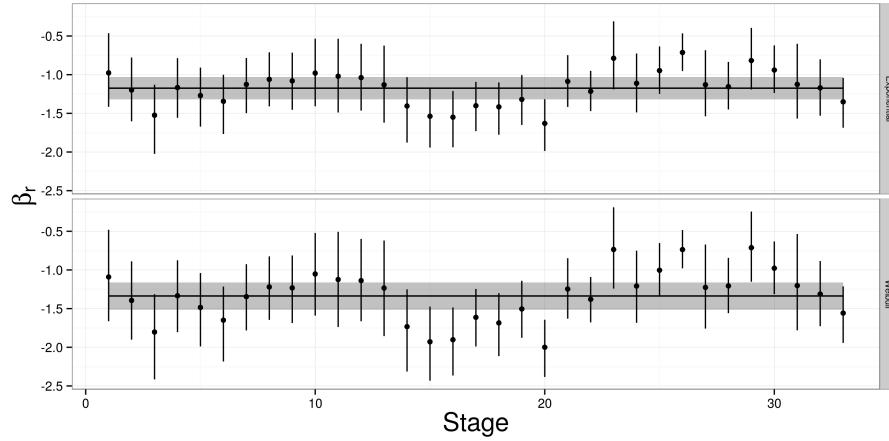


Figure 8: Comparison of cohort-specific estimates of the effect of geographic range on extinction risk β_r , presented along with the estimate for the overall effect of geographic range. Points correspond to the median of the cohort-specific estimate, along with 80% credible intervals. The horizontal line is the median estimate of the overall baseline extinction risk along with 80% credible intervals. Results are presented for the exponential (top) and Weibull (bottom) models.

440 Taxon traits like environmental preference or geographic range (Hunt et al.,
2005, Jablonski, 1987) are most likely heritable, at least phylogenetically
442 (Housworth et al., 2004, Lynch, 1991). Without phylogenetic context, this
analysis assumes that differences in extinction risk between taxa are
444 independent of those taxa's shared evolutionary history (Felsenstein, 1985). In
contrast, the origination cohorts only capture shared temporal context. The
446 inclusion of phylogenetic context as an addition individual level hierarchical
structure independent of origination cohort would allow for determining how
448 much of the observed variability is due to shared evolutionary history versus
actual differences associated with these taxonomic traits. For example, it has
450 been shown that phylogeny contribute non-trivially to differences in mammal
species durations SMITS IN PREP.

452 In summary, patterns of Paleozoic brachiopod survival were analyzed using a

fully Bayesian hierarchical survival modelling approach. Using a varying-slopes,
454 varying-intercepts approach I am able to model both the overall mean effect of
biological covariates on extinction risk while also modeling the correlation
456 between origination cohort-specific estimates of covariate effects. I find that as
baseline extinction risk increases, the strength of the selection gradient on
458 biological traits (except body size) increases. This manifests as greater
differences in extinction risk for each unit difference in the biological covariates
460 during periods of high extinction risk, while a much flatter total selection
gradient during periods of low extinction risk. I also find some support for
462 “survival of the unspecialized” (Liow, 2004, 2007, Nürnberg and Aberhan, 2013,
2015, Simpson, 1944) as a general characterization of the effect of environmental
464 preference on extinction risk (Fig. 3), though there is heterogeneity between
origination cohorts (Fig. 9). Generally, this study demonstrates the advantages
466 of a hierarchical Bayesian framework for taking into account the structured
nature of the data. Future studies of structured data should adopt similar
468 strategies in order to best model our knowledge instead of ignoring that
structure which can lead to poor and/or incorrect inference.

470 Acknowledgements

I would like to thank K. Angielczyk, M. Foote, P. D. Polly, and R. Ree for
472 helpful discussion and advice. Additionally, thank you A. Miller for the
epicontinental versus open-ocean assignments. This entire study would would
474 not have been possible without the Herculean effort of the many contributors to
the Paleobiology Database. In particular, I would like to thank NAMES. This is
476 Paleobiology Database publication XXX.

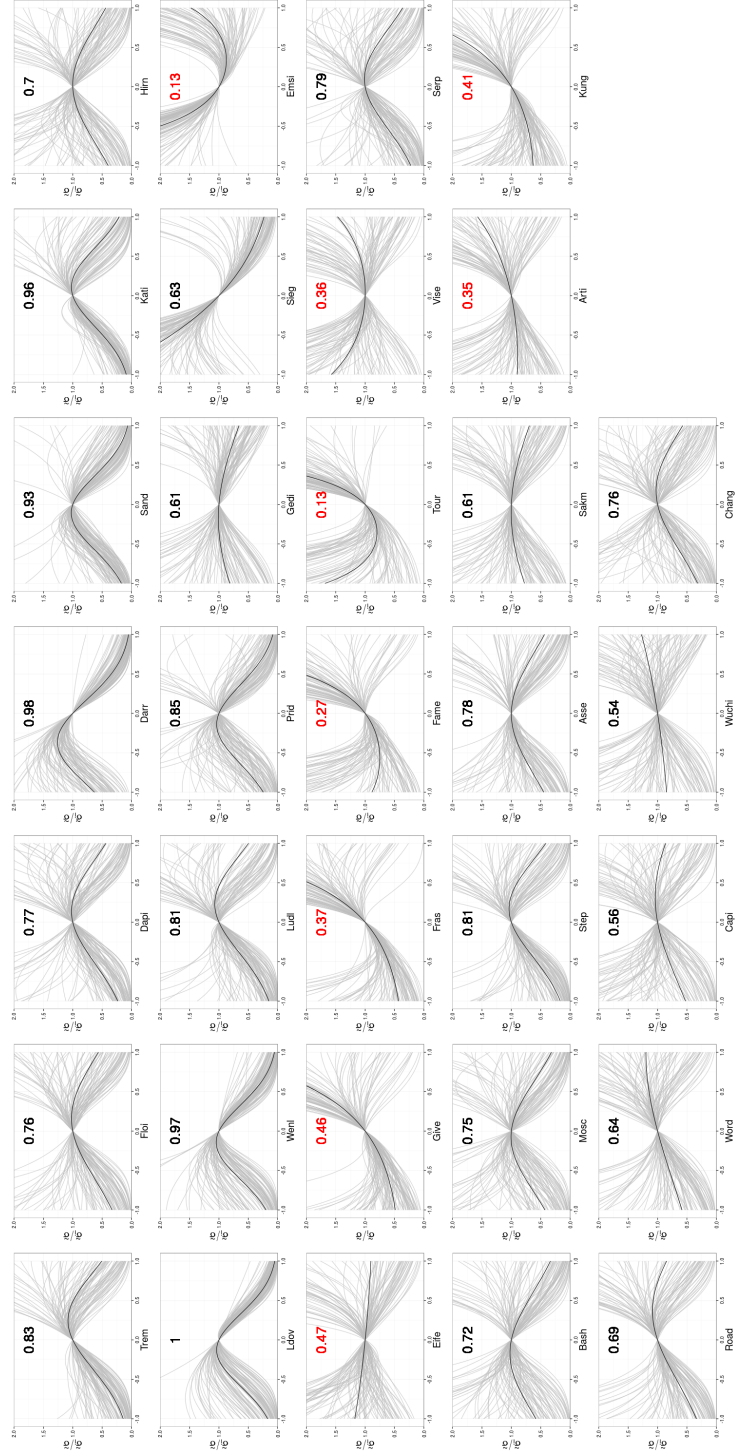


Figure 9: Comparison of the cohort-specific estimates of $f(v_i)$ (Eq. 3) for the 33 analyzed origination cohorts. The stage of origination is labeled on the x-axis of each panel. The oldest stage is in the upper left, while the youngest is in the lower left. The number in each panel corresponds to the posterior probability that $f(v_i)$ is concave down. Those that are highlighted in red have less than 51% posterior predictive probability that $f(v_i)$ is concave down.

References

- Alexander, R. R., 1977. Generic longevity of articulate brachiopods in relation to the mode of stabilization on the substrate. *Palaeogeography, Palaeoclimatology, Palaeoecology* 21:209–226.
- Baumiller, T. K., 1993. Survivorship analysis of Paleozoic Crinoidea: effect of filter morphology on evolutionary rates. *Paleobiology* 19:304–321.
- Carvalho, C. M., N. G. Polson, and J. G. Scott, 2009. Handling Sparsity via the Horseshoe. *in* *Proceedings of the 12th International Conference on Artificial Intelligence and Statistics*, vol. 5, Pp. 73–80.
- , 2010. The horseshoe estimator for sparse signals. *Biometrika* 97:465–480. URL <http://biomet.oxfordjournals.org/cgi/doi/10.1093/biomet/asq017>.
- Cooper, W. S., 1984. Expected time to extinction and the concept of fundamental fitness. *Journal of Theoretical Biology* 107:603–629.
- Felsenstein, J., 1985. Phylogenies and the comparative method. *American Naturalist* 125:1–15. URL <http://www.jstor.org/stable/2461605>.
- Foote, M., 1988. Survivorship analysis of Cambrian and Ordovician Trilobites. *Paleobiology* 14:258–271.
- , 2006. Substrate affinity and diversity dynamics of Paleozoic marine animals. *Paleobiology* 32:345–366. URL <http://www.bioone.org/doi/abs/10.1666/05062.1>.
- Foote, M. and A. I. Miller, 2013. Determinants of early survival in marine animal genera. *Paleobiology* 39:171–192. URL <http://www.bioone.org/doi/abs/10.1666/12028>.

502 Gelman, A., 2006. Prior distributions for variance parameters in hierarchical
models. *Bayesian Analysis* 1:515–533.

504 Gelman, A., J. B. Carlin, H. S. Stern, D. B. Dunson, A. Vehtari, and D. B.
Rubin, 2013. *Bayesian data analysis*. 3 ed. Chapman and Hall, Boca Raton,
FL.

506 Gelman, A. and J. Hill, 2007. *Data Analysis using Regression and
Multilevel/Hierarchical Models*. Cambridge University Press, New York, NY.

508 Hijmans, R. J., 2015. raster: Geographic data analysis and modeling. URL
<http://CRAN.R-project.org/package=raster>. R package version 2.3-24.

510 Hoffman, M. D. and A. Gelman, 2014. The No-U-Turn Sampler: Adaptively
Setting Path Lengths in Hamiltonian Monte Carlo. *Journal of Machine
Learning Research* 15:1351–1381.

512 Housworth, E. A., P. Martins, and M. Lynch, 2004. The Phylogenetic Mixed
Model. *The American Naturalist* 163:84–96.

514 Hunt, G., K. Roy, and D. Jablonski, 2005. Species-level heritability reaffirmed: a
comment on "On the heritability of geographic range sizes". *American
Naturalist* 166:129–135.

518 Ibrahim, J. G., M.-H. Chen, and D. Sinha, 2001. *Bayesian Survival Analysis*.
Springer, New York.

520 Jablonski, D., 1986. Background and mass extinctions: the alternation of
macroevolutionary regimes. *Science* 231:129–133.

522 ———, 1987. Heritability at the species level: analysis of geographic ranges of
cretaceous mollusks. *Science* 238:360–363. URL
524 <http://www.ncbi.nlm.nih.gov/pubmed/17837117>.

- Jablonski, D. and K. Roy, 2003. Geographical range and speciation in fossil and
526 living
molluscs. *Proceedings. Biological sciences / The Royal Society* 270:401–6. URL
528 <http://www.pubmedcentral.nih.gov/articlerender.fcgi?artid=1691247&tool=pmcentrez&rendertype>
- Johnson, J. G., 1974. Extinction of Perched Faunas. *Geology* 2:479–482.
- 530 Kiessling, W. and M. Aberhan, 2007. Environmental determinants of marine
benthic biodiversity dynamics through Triassic–Jurassic time. *Paleobiology*
532 33:414–434.
- Klein, J. P. and M. L. Moeschberger, 2003. *Survival Analysis: Techniques for*
534 *Censored and Truncated Data*. 2nd ed. Springer, New York.
- Liow, L. H., 2004. A test of Simpson’s ”rule of the survival of the relatively
536 unspecialized” using fossil crinoids. *The American naturalist* 164:431–43.
URL <http://www.ncbi.nlm.nih.gov/pubmed/15459876>.
- 538 ———, 2007. Does versatility as measured by geographic range, bathymetric
range and morphological variability contribute to taxon longevity? *Global*
540 *Ecology and Biogeography* 16:117–128. URL
<http://doi.wiley.com/10.1111/j.1466-8238.2006.00269.x>
542 [papers2://publication/doi/10.1111/j.1466-8238.2006.00269.x](http://doi.wiley.com/10.1111/j.1466-8238.2006.00269.x).
- Lynch, M., 1991. Methods for the analysis of comparative data in evolutionary
544 biology. *Evolution* 45:1065–1080.
- Miller, A. I. and S. R. Connolly, 2001. Substrate affinities of higher taxa and
546 the Ordovician Radiation. *Paleobiology* 27:768–778. URL
<http://www.bioone.org/doi/abs/10.1666/0094-8373%282001%29027%3C0768%3ASAOHTA%3E2.O.CO%3B2>.
- 548 Miller, A. I. and M. Foote, 2009. Epicontinental seas versus open-ocean settings:

- the kinetics of mass extinction and origination. *Science* 326:1106–9. URL
550 <http://www.ncbi.nlm.nih.gov/pubmed/19965428>.
- Nürnberg, S. and M. Aberhan, 2013. Habitat breadth and geographic range
552 predict diversity dynamics in marine Mesozoic bivalves. *Paleobiology*
39:360–372. URL <http://www.bioone.org/doi/abs/10.1666/12047>.
- , 2015. Interdependence of specialization and biodiversity in Phanerozoic
554 marine invertebrates. *Nature communications* 6:6602. URL
556 <http://www.ncbi.nlm.nih.gov/pubmed/25779979>.
- Palmer, M. E. and M. W. Feldman, 2012. Survivability is more fundamental
558 than evolvability. *PloS one* 7:e38025. URL
<http://www.pubmedcentral.nih.gov/articlerender.fcgi?artid=3377627&tool=pmcentrez&rendertype>
- 560 Payne, J. L. and S. Finnegan, 2007. The effect of geographic range on
extinction risk during background and mass extinction. *Proceedings of the*
562 *National Academy of Sciences* 104:10506–11. URL
<http://www.pubmedcentral.nih.gov/articlerender.fcgi?artid=1890565&tool=pmcentrez&rendertype>
- 564 Payne, J. L., N. A. Heim, M. L. Knope, and C. R. McClain, 2014. Metabolic
dominance of bivalves predates brachiopod diversity decline by more than 150
566 million years. *Proceedings of the Royal Society B* 281:20133122.
- Peters, S. E., 2008. Environmental determinants of extinction selectivity in the
568 fossil record. *Nature* 454:626–9. URL
<http://www.ncbi.nlm.nih.gov/pubmed/18552839>.
- 570 Raup, D. M., 1975. Taxonomic survivorship curves and Van Valen’s Law.
Paleobiology 1:82–96. URL
572 <http://www.ncbi.nlm.nih.gov/pubmed/17777225>.
- , 1978. Cohort Analysis of generic survivorship. *Paleobiology* 4:1–15.

- 574 Sepkoski Jr., J. J., 1981. A factor analytic description of the Phanerozoic
marine fossil record. *Paleobiology* 7:36–53.
- 576 Sheehan, P., 2001. The late Ordovician mass extinction. *Annual Review of*
Earth and Planetary Sciences 29:331–364. URL
578 <http://www.annualreviews.org/doi/abs/10.1146/annurev.earth.29.1.331>.
- Simpson, C., 2006. Levels of selection and large-scale morphological trends.
580 Ph.D. thesis, University of Chicago.
- Simpson, C. and P. G. Harnik, 2009. Assessing the role of abundance in marine
582 bivalve extinction over the post-Paleozoic. *Paleobiology* 35:631–647. URL
<http://www.bioone.org/doi/abs/10.1666/0094-8373-35.4.631>.
- 584 Simpson, G. G., 1944. *Tempo and Mode in Evolution*. Columbia University
Press, New York.
- 586 ———, 1953. *The Major Features of Evolution*. Columbia University Press,
New York.
- 588 Stan Development Team, 2014a. Stan: A c++ library for probability and
sampling, version 2.5.0. URL <http://mc-stan.org/>.
- 590 ———, 2014b. Stan Modeling Language Users Guide and Reference Manual,
Version 2.5.0. URL <http://mc-stan.org/>.
- 592 Van Valen, L., 1973. A new evolutionary law. *Evolutionary Theory* 1:1–30.
URL <http://ci.nii.ac.jp/naid/10011264287/>.
- 594 ———, 1979. Taxonomic survivorship curves. *Evolutionary Theory* 4:129–142.
- Wang, S. C., 2003. On the continuity of background and mass extinction.
596 *Paleobiology* 29:455–467. URL
<http://www.bioone.org/doi/abs/10.1666/0094-8373%282003%29029%3C0455%3AOTCOBA%3E2.0.CO%3B2>.

598 Watanabe, S., 2010. Asymptotic Equivalence of Bayes Cross Validation and
Widely Applicable Information Criterion in Singular Learning Theory.
600 Journal of Machine Learning Research 11:3571–3594.

A Uncertainty in environmental preference

602 The calculation and inclusion of environmental affinity in the survival model is a
statistical procedure that takes into account our uncertainty based on where
604 fossils tend to occur. Because we cannot directly observe if a fossil taxon had
occurrences restricted to only a single environment, instead we can only
606 estimate its affinity with uncertainty. One advantage of using a Bayesian
analytical approach is that both parameters and data are considered random
608 samples from some underlying distribution, which means that it is possible to
model the uncertainty in our covariates of interest (Gelman et al., 2013). My
610 approach is conceptually similar to Simpson and Harnik (2009) but instead of
obtaining a single point estimate, an entire posterior distribution is estimated.

612 The first step is to determine the probability θ at which genus i occurs in an
epicontinental settings based on its own pattern of occurrences. Define e_i as the
614 number of occurrences of genus i in an epicontinental sea and o_i as the number of
occurrences of genus i not in an epicontinental sea (e.g. open ocean). Because
616 the value of interest is the probability of occurring in an epicontinental
environment, given the observed fossil record, I assume that probability follows
618 a binomial distribution. We can then define our sampling statement as

$$e_i \sim \text{Binomial}(e_i + o_i, \theta_i). \quad (4)$$

I used a flat prior for θ_i defined as $\theta_i \sim \text{Beta}(1, 1)$. Because the beta
620 distribution is the conjugate prior for the binomial distribution, the posterior is
easy to compute in closed form. The posterior probability of θ is then

$$\theta_i \sim \text{Beta}(e_i + 1, o_i + 1) \quad (5)$$

622 It is extremely important, however, to take into account the overall
 environmental occurrence probability of all other genera present at the same
 624 time as genus i . This is incorporated as an additional probability Θ . Define E_i
 as the total number of other fossil occurrences (except for genus i) in
 626 epicontinental seas during stages where i occurs and O_i as the number of other
 fossil occurrences not on epicontinental seas. We can then define the sampling
 628 statement as

$$E_i \sim \text{Binomial}(E_i + O_i, \Theta_i). \quad (6)$$

Again, I used a flat prior of Θ_i defined as $\Theta_i \sim \text{Beta}(1, 1)$. The posterior of Θ is
 630 then simply defined as

$$\Theta_i \sim \text{Beta}(E_i + 1, O_i + 1) \quad (7)$$

I then define the environmental affinity of genus i as $v_i = \theta_i - \Theta_i$. v_i is a value
 632 that can range between -1 and 1, where negative values indicate that genus i
 tends to occur more frequently in open ocean environments than background
 634 while positive values indicate that genus i tends to occur in epicontinental
 environments.

636 While this approach is noticeably more complicated than previous ones (Foote,
 2006, Kiessling and Aberhan, 2007, Miller and Connolly, 2001, Simpson and
 638 Harnik, 2009) there are some important benefits to both using a continuous
 measure of affinity as well directly modeling our uncertainty. In order to show
 640 some of these benefits, I performed a simulation analysis of how
 modal/maximum *a posteriori* (MAP) estimates versus full posterior estimates.

642 In this simulation, I first defined the “background” epicontinental occurrence θ_b
 as 0.50 with a small amount of noise. This was represented as a beta distribution

$$\Theta_b = \text{Beta}(\alpha = 2500, \beta = 2500). \quad (8)$$

644 This choice of parameters for the distribution reflects the average number of
background occurrences for either epicontinental or open ocean environments
646 per genus.

Using this background occurrence ratio, I randomly generated the occurrence
648 patterns of 1000 simulated taxa. This was done at multiple sample sizes (1, 2, 3,
4, 5, 10, 25, 50, 100) in order to demonstrate the effects of increasing sample
650 size on the confidence of environmental affinity. For each simulated taxon I
calculated the full posterior distribution while assuming a flat Beta prior
652 (Beta(1, 1)). Using the full posterior I calculated the MAP probability of
occurring in epicontinental environments. The environmental affinity was
654 calculated for each of the simulated taxa using both the full posterior and the
MAP estimate. In this toy example, environmental affinity can range between
656 -0.5 and 0.5.

As should be expected, as sample size increases the distribution of MAP
658 estimates converge on the true value (Fig. 10). For taxa with less than 10
occurrences, the MAP estimate is biased towards extreme values. Note that the
660 mode of the beta distribution is not defined for situations where there were 0
draws of one of the environmental conditions. Instead, the vertical line is based
662 entirely on the observed occurrences which are technically the modal estimates
because they are the most frequently occurring/highest density.

664 In contrast, we can compare the true occurrence probability distribution versus
the posterior estimate for a given sample (Fig. 11). When sample sizes are low,
666 posterior estimates are flat and represent a compromise between the likelihood
and the flat prior (Eq. 5). Because of this, estimates from small sizes are less

likely to be overly biased towards the extremes. This is further emphasized by inspection of the estimates of environmental affinity for the simulated taxa (Fig. 12). Posterior estimates from simulated taxa with small sample size have a much broader distribution that both allows for the extreme observation but still captures the “true” value (0).

By defining environmental preference as the difference in full posterior estimates of occurrence probability, it is possible to include taxa with low sample sizes that are normally discarded (Foote, 2006, Kiessling and Aberhan, 2007, Miller and Connolly, 2001, Simpson and Harnik, 2009). Additionally, 55+% of observed Paleozoic brachiopod genera have less than 10 occurrences which is the range of sample sizes where MAP (or ML) estimates would be potentially most biased. This is preferable to finding the difference between the MAP estimates (blue line; Fig. 12).

B Survival model

The simplest model of genus duration includes no covariate or structural information. Define y_i as the duration in stages of genus i , where $i = 1, \dots, n$ and n is the number of observed genera. These two models are then simply defined as

$$\begin{aligned} y_i &\sim \text{Exponential}(\lambda) \\ y_i &\sim \text{Weibull}(\alpha, \sigma). \end{aligned} \tag{9}$$

λ, α , and σ are all defined for all positive reals. Note that λ is a “rate” or inverse-scale while σ is a scale parameter, meaning that $\frac{1}{\lambda} = \sigma$.

These simple models can then be expanded to include covariate information as predictors by reparameterizing λ or σ as a regression (Klein and Moeschberger,

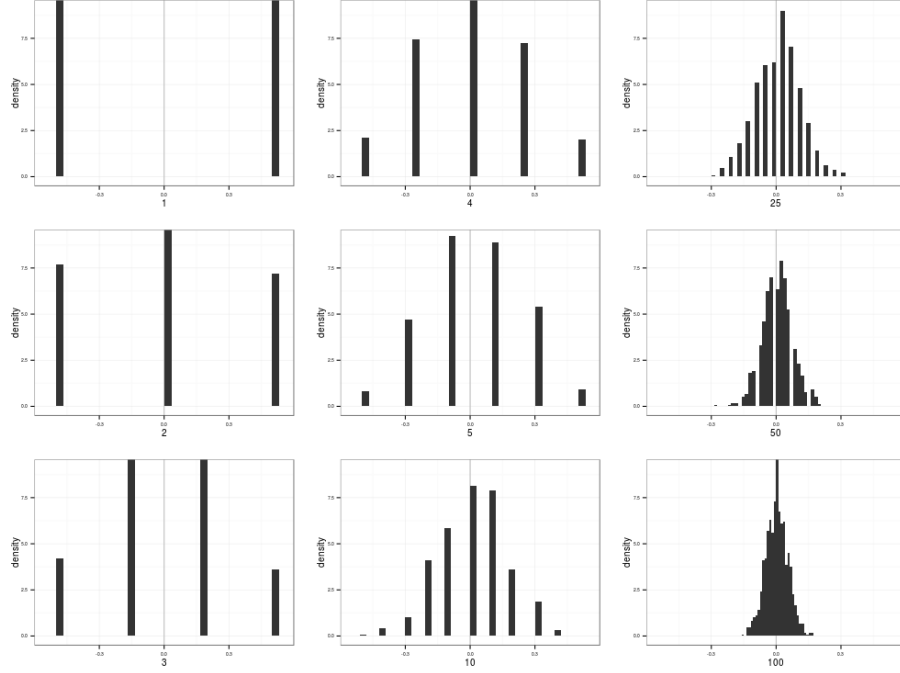


Figure 10: Histograms of the distributions of from the beta distribution defined in Eq. 8. As to be expected, as sample size increases the draws better resemble the underlying true distribution. Sample size is indicated as the label of the x-axis, increasing in column major order.

2003). Each of the covariates of interest is given its own regression coefficient (e.g. β_r) along with an intercept term β_0 . There are some additional complications to the parameterization of σ associated with the inclusion of α as well as for interpretability (Klein and Moeschberger, 2003). Both of these are then written as

$$\begin{aligned}\lambda_i &= \exp(\beta_0 + \beta_r r_i + \beta_v v_i + \beta_{v^2} v_i^2 + \beta_m m_i) \\ \sigma_i &= \exp\left(\frac{-(\beta_0 + \beta_r r_i + \beta_v v_i + \beta_{v^2} v_i^2 + \beta_m m_i)}{\alpha}\right).\end{aligned}\tag{10}$$

The quadratic term for environmental affinity v is to allow for the possible nonlinear relationship between environmental affinity and extinction risk.

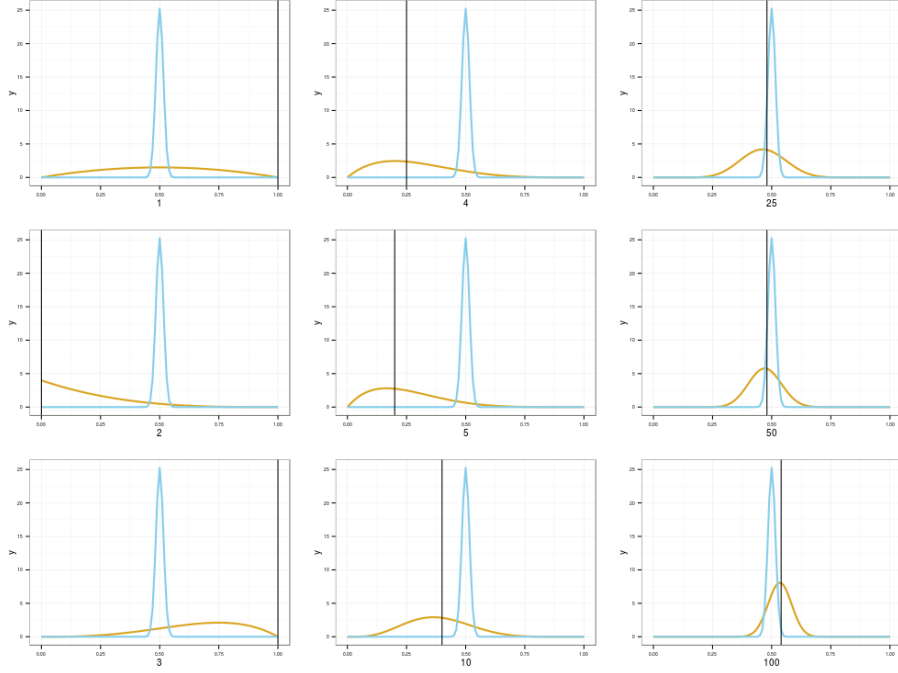


Figure 11: Comparisons of the underlying distribution (blue) to posterior estimates based on increasing sample size (gold). Each posterior estimate is represented for only a single realization of draws, each with sample size indicated as the x-axis label (increasing in column major order). Black vertical lines correspond to the MAP estimate of the simulated taxon’s affinity. This stands in contrast to the posterior distribution of expected affinity in gold.

The models which incorporate both equations 9 and 10 can then be further
698 expanded to allow all of the β coefficients, including β_0 , to vary with origination
cohort while also modeling their covariance and correlation. This is called a
700 varying-intercepts, varying-slopes model (Gelman and Hill, 2007). It is much
easier to represent and explain how this is parameterized using matrix notation.
702 First, define \mathbf{B} as $k \times J$ matrix of the k coefficients including the intercept term
($k = 5$) for each of the J cohorts. Second, define \mathbf{X} as a $n \times k$ matrix where each
704 column is one of the covariates of interest. Importantly, \mathbf{X} includes a columns of
all 1s which correspond to the constant term β_0 . Third, define $j[i]$ as the

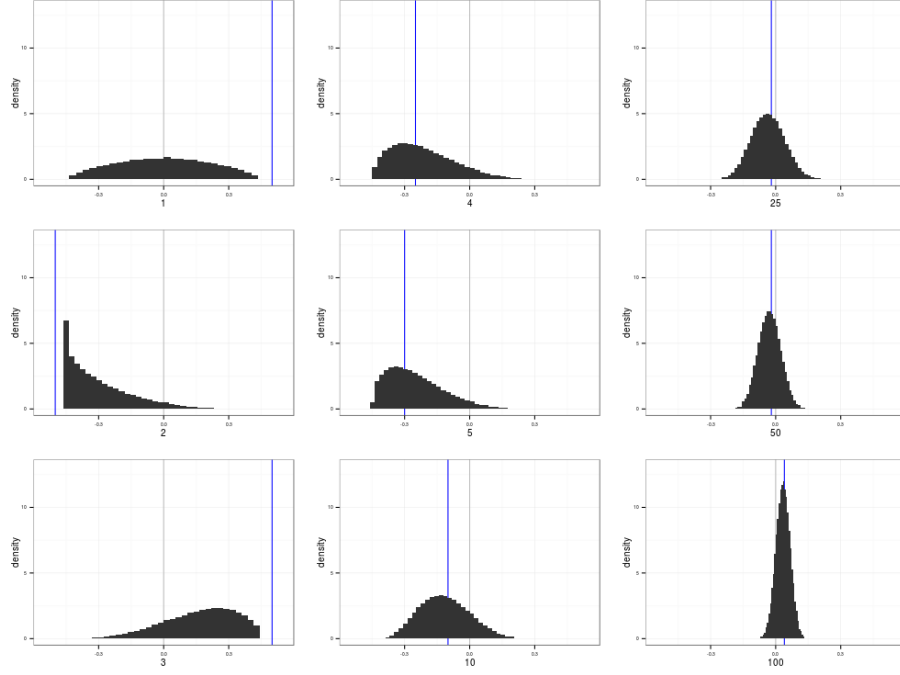


Figure 12: Histograms of the difference in the underlying occurrence distribution and the posterior distribution estimates from the previous graph (Fig. 11). The “true” value is included in all distributions of environmental affinities. Each affinity estimate is represented for only a single realization of draws, each with sample size indicated as the x-axis label (increasing in column major order). Blue vertical lines correspond to the difference in MAP estimates between the underlying distribution and the simulated taxon’s draws. This stands in contrast to the distribution of the differences between the simulated taxon and background.

706 origination cohort of genus i , where $j = 1, \dots, J$ and J is the total number of
observed cohorts. We then rewrite λ and σ of equation 10 in matrix notation as

$$\begin{aligned}\lambda_i &= \exp(\mathbf{X}_i B_{j[i]}) \\ \sigma_i &= \exp\left(\frac{-(\mathbf{X}_i B_{j[i]})}{\alpha}\right).\end{aligned}\tag{11}$$

708 Because B is a matrix, I use a multivariate normal prior with unknown vector

of means μ and covariance matrix Σ . This is written as

$$B \sim \text{MVN}(\vec{\mu}, \Sigma) \quad (12)$$

710 where $\vec{\mu}$ is length k vector representing the overall mean of the distributions of
 β coefficients. Σ is a $k \times k$ covariance matrix of the β coefficients.

712 What remains is assigning priors the elements of $\vec{\mu}$ and the covariance matrix Σ .
 All elements of $\vec{\mu}$ except for μ_r were given horseshoe priors (Carvalho et al.,
 714 2009, 2010) while μ_r was given an informative normal prior ($\mu_r \sim \mathcal{N}(-1, 1)$).
 Horseshoe priors are a strong regularizing priors with effectively infinite density
 716 at 0 and heavy, Cauchy-like tails (Carvalho et al., 2009, 2010) which allow
 weakly inferred effects to be strongly drawn towards 0 while truly strong effects
 718 can remain large.

The prior for Σ is a bit more complicated due to its multivariate nature.

720 Following the Stan Development Team (2014b), I modeled the scale terms
 separate from the correlation structure of the coefficients. This is possible
 722 because of the relationship between a covariance and a correlation matrix,
 defined as

$$\Sigma_B = \text{Diag}(\vec{\tau})\Omega\text{Diag}(\vec{\tau}) \quad (13)$$

724 where $\vec{\tau}$ is a length k vector of variances and $\text{Diag}(\tau)$ is a diagonal matrix.

I used a LKJ prior distribution for correlation matrix Ω as recommended by
 726 Stan Development Team (2014b). The LKJ distribution is a single parameter
 multivariate distribution where values of the parameter η greater than 1
 728 concentrate density at the unit correlation matrix, which corresponds to no
 correlation between the β coefficients. The scale parameters, $\vec{\tau}$, are given weakly
 730 informative half-Cauchy (C^+) priors following Gelman (2006).

C Censored observations

732 A key aspect of survival analysis is the inclusion of censored, or incompletely
observed, data points (Ibrahim et al., 2001, Klein and Moeschberger, 2003). The
734 two classes of censored observations encountered in this study were right and
left censored observations. Right censored genera are those that did not go
736 extinct during the window of observation, or genera that are still extant. Left
censored observations are those taxa for which we know only an upper limit on
738 their duration.

In the context of this study, I considered all genera that had a duration of only
740 one geologic stage to be left censored as we do not have a finer degree of
resolution.

742 The key function for modeling censored observations is the survival function, or
 $S(t)$. $S(t)$ corresponds to the probability that a genus having existed for t stages
744 will not have gone extinct while $h(t)$ corresponds to the instantaneous
extinction rate at taxon age t Klein and Moeschberger (2003). For an
746 exponential model, $S(t)$ is defined as

$$S(t) = \exp(-\lambda t), \quad (14)$$

and for the Weibull distribution $S(t)$ is defined as

$$S(t) = \exp\left(-\left(\frac{t}{\sigma}\right)^\alpha\right). \quad (15)$$

748 $S(t)$ is equivalent to the complementary cumulative distribution function,
 $1 - F(t)$ (Klein and Moeschberger, 2003).

750 For right censored observations, instead of calculating the likelihood as normal

(Eq. 11) the likelihood of an observation is evaluated using $S(t)$. Conceptually,
 752 this approach calculates the likelihood of observing a taxon that existed for at
 least that long. For left censored data, instead the likelihood is calculated using
 754 $1 - S(t)$ which corresponds to the likelihood of observing a taxon that existed
 no longer than t .

756 The full likelihood statements incorporating fully observed, right censored, and
 left censored observations are then

$$\begin{aligned}\mathcal{L} &\propto \prod_{i \in C} \text{Exponential}(y_i | \lambda) \prod_{j \in R} S(y_j | \lambda) \prod_{k \in L} (1 - S(y_k | \lambda)) \\ \mathcal{L} &\propto \prod_{i \in C} \text{Weibull}(y_i | \alpha, \sigma) \prod_{j \in R} S(y_j | \alpha, \sigma) \prod_{k \in L} (1 - S(y_k | \alpha, \sigma))\end{aligned}\tag{16}$$

758 where C is the set of all fully observed taxa, R the set of all right censored taxa,
 and L the set of all left-censored taxa.

760 D Widely applicable information criterion

WAIC can be considered a fully Bayesian alternative to the Akaike information
 762 criterion, where WAIC acts as an approximation of leave-one-out
 cross-validation which acts as a measure of out-of-sample predictive accuracy
 764 (Gelman et al., 2013). WAIC is calculated starting with the log pointwise
 posterior predictive density calculated as

$$\text{lppd} = \sum_{i=1}^n \log \left(\frac{1}{S} \sum_{s=1}^S p(y_i | \Theta^s) \right), \tag{17}$$

766 where n is sample size, S is the number posterior simulation draws, and Θ
 represents all of the estimated parameters of the model. This is similar to
 768 calculating the likelihood of each observation given the entire posterior. A

correction for the effective number of parameters is then added to lppd to
770 adjust for overfitting. The effective number of parameters is calculated,
following the recommendations of Gelman et al. (2013), as

$$p_{\text{WAIC}} = \sum_{i=1}^n V_{s=1}^S (\log p(y_i | \Theta^S)). \quad (18)$$

772 where V is the sample posterior variance of the log predictive density for each
data point.

774 Given both equations 17 and 18, WAIC is then calculated

$$\text{WAIC} = \text{lppd} - p_{\text{WAIC}}. \quad (19)$$

When comparing two or more models, lower WAIC values indicate better
776 out-of-sample predictive accuracy. Importantly, WAIC is just one way of
comparing models. When combined with posterior predictive checks it is
778 possible to get a more complete understanding of a model's fit to the data.